

## Three-Dimensional Cage Type Mesoporous CN-Based Hybrid Material with Very High Surface Area and Pore Volume

Ajayan Vinu,<sup>\*,†</sup> Pavuluri Srinivasu,<sup>†</sup> Dhanashri P. Sawant,<sup>†</sup> Toshiyuki Mori,<sup>†</sup>  
Katsuhiko Ariga,<sup>‡</sup> Jong-San Chang,<sup>§</sup> Sung-Hwa Jung,<sup>§</sup>  
Veerappan Vaithilingam Balasubramanian,<sup>†</sup> and Young Kyu Hwang<sup>§</sup>

Nano Ionics Materials Group and Supermolecules Group, National Institute for Materials Science, 1-1 Namiki, Tsukuba, Ibaraki 305-0044, Japan, and Catalysis Center for Molecular Engineering, Korea Research Institute of Chemical Technology, Yusong-ku, Taejeon 305-606, South Korea

Received March 9, 2007. Revised Manuscript Received June 26, 2007

A novel highly ordered three-dimensional mesoporous carbon-nitride-based hybrid material (MCN-2) with very high surface area, pore volume, and a possible cage type porous structure has been prepared using three-dimensional cage type mesoporous silica, SBA-16, as a template through a simple polymerization reaction between ethylenediamine and carbon tetrachloride. The material has been unambiguously characterized by various sophisticated techniques such as XRD, nitrogen adsorption, HRTEM, EELS, XPS, 13C DD-MAS, and FT-IR spectroscopy. The XRD result reveals that MCN-2 possesses three-dimensional structure with a possible *Im3m* space group. The specific surface area and pore volume of MCN-2 are significantly higher as compared to those of the template and MCN-1. Because of the excellent textural characteristic and three-dimensional porous structure, we believe that the MCN-2 could offer great potential for the applications such as catalysis and adsorption.

### Introduction

Mesoporous materials with cage type three-dimensional porous structure, namely, SBA-1, SBA-6, and SBA-16, have attracted a significant attention in recent days because of their excellent textural characteristics.<sup>1–3</sup> Among the cage type mesoporous materials, SBA-16, synthesized using a low-cost polymeric F127 surfactant, has received much attention because of its three-dimensional structure with a large cage type mesopores of diameter well above 5 nm, thicker pore walls, and excellent thermal and mechanical stabilities. This material has a body-centered cubic porous structure with eight nearest-neighbor mesopores, which are connected to each other by their adjacent mesopores.<sup>1–4</sup> The above interesting structural features make it useful for many applications, including catalysis, adsorption, and separation. Several researchers have tried to make a cage type mesoporous carbon using SBA-16 as a hard template. However, most of them failed to get a well-ordered mesoporous carbon because of narrow pore aperture between the adjacent cages of SBA-16. Recently, Kim et al. have successfully prepared a cage type mesoporous carbon material from SBA-16 by using a small size carbon precursor, such as furfuryl alcohol.<sup>5</sup>

Carbon nitride (CN) is a well-known and interesting material that has attracted worldwide attention because the incorporation of nitrogen atoms in the carbon nanostructure can enhance the mechanical, conducting, field-emission, and energy-storage properties.<sup>6–19</sup> CN materials with five different structures have been predicted so far: one is two-dimensional graphitic C<sub>3</sub>N<sub>4</sub>, and four are three-dimensional carbon nitrides, namely,  $\alpha$ -C<sub>3</sub>N<sub>4</sub>,  $\beta$ -C<sub>3</sub>N<sub>4</sub>, cubic C<sub>3</sub>N<sub>4</sub>, and pseudocubic C<sub>3</sub>N<sub>4</sub>. Among the CN materials,  $\beta$ -C<sub>3</sub>N<sub>4</sub> and its allotropic cubic and pseudocubic phases are superhard materials whose structure and properties are expected to be similar to those of diamond and  $\beta$ -Si<sub>3</sub>N<sub>4</sub>.<sup>20,21</sup> Groenewolt and

\* To whom correspondence should be addressed. Phone: 81-29-860-4563. Fax: 81-29-860-4667. E-mail: vinu.ajayan@nims.go.jp.

<sup>†</sup> Nano Ionics Materials Group, National Institute for Materials Science.

<sup>‡</sup> Supermolecules Group, National Institute for Materials Science.

<sup>§</sup> Korea Research Institute of Chemical Technology.

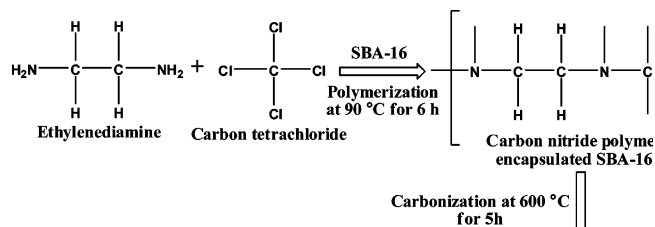
- (1) Sakamoto, Y.; Kaneda, M.; Terasaki, O.; Zhao, D.; Kim, J. M.; Stucky, G.; Shin, H. J.; Ryoo, R. *Nature* **2000**, *408*, 449.
- (2) Vinu, A.; Murugesan, V.; Hartmann, M. *Chem. Mater.* **2003**, *15*, 1385.
- (3) Zhao, D.; Feng, J.; Huo, Q.; Melosh, N.; Fredrikson, G.; Chmelka, B.; Stucky, G. D. *Science* **1998**, *279*; Zhao, D.; Huo, Q.; Feng, J.; Chmelka, B. F.; Stucky, G. D. *J. Am. Chem. Soc.* **1998**, *120*, 6024.
- (4) Kim, T.-W.; Ryoo, R.; Kruk, M.; Gierszal, K. P.; Jaroniec, M.; Kamiya, S.; Terasaki, O. *J. Phys. Chem. B* **2004**, *108*, 11480.

- (5) Kim, T.-W.; Ryoo, R.; Gierszal, K. P.; Jaroniec, M.; Solovyov, L. A. *J. Mater. Chem.* **2005**, *15*, 1560.
- (6) Kawaguchi, M.; Yagi, S.; Enomoto, H. *Carbon* **2004**, *42*, 345.
- (7) Khabashesku, V. N.; Zimmerman, J. L.; Margrave, J. L. *Chem. Mater.* **2000**, *12*, 3264.
- (8) Qiu, Y.; Gao, L. *Chem. Commun.* **2003**, 2378.
- (9) Sánchez-López, J. C.; Donnet, C.; Lefebvre, F.; Fernández-Ramos, C.; Fernández, A. *J. Appl. Phys.* **2001**, *90*, 675.
- (10) Marton, D.; Boyd, K. J.; Al-Bayati, A. H.; Todorov, S. S.; Rabalais, J. W. *Phys. Rev. Lett.* **1994**, *73*, 118.
- (11) Chen, Y. H.; Tay, B. K.; Lau, S. P.; Shi, X.; Qiao, X. L.; Chen, J. G.; Wu, Y. P.; Sun, Z. H.; Xie, C. S. *J. Mater. Res.* **2002**, *17*, 521.
- (12) Hellgren, N.; Guo, J.; Luo, Y.; Sâthe, C.; Agui, A.; Kashtanov, S.; Nordgren, J.; Ågren, H.; Sundgren, J. E. *Thin Solid Films* **2005**, *471*, 19.
- (13) Kroke, E.; Schwarz, M. *Coord. Chem. Rev.* **2004**, *248*, 493.
- (14) Guo, Q.; Yang, Q.; Zhu, L.; Yi, C.; Zhang, S.; Xie, Y. *Solid State Commun.* **2004**, *132*, 369.
- (15) Bai, Y.-J.; Lu, B.; Liu, Z.-G.; Li, L.; Cui, D.-L.; Xu, X.-G.; Wang, Q.-L. *J. Cryst. Growth* **2003**, *247*, 505.
- (16) Zimmerman, J. L.; Williams, R.; Khabashesku, V. N.; Margrave, J. L. *Nano Lett.* **2001**, *12*, 731.
- (17) Gillan, E. G. *Chem. Mater.* **2000**, *12*, 3906.
- (18) Kouvetakis, J.; Bandari, A.; Todd, M.; Wilkens, B.; Cave, N. *Chem. Mater.* **1994**, *6*, 811.
- (19) Wang, J.; Miller, D. R.; Gillan, E. G. *Carbon* **2003**, *41*, 2031.
- (20) Cohen, M. L. *Phys. Rev. B* **1985**, *32*, 7988.

Antonietti reported that the nanoparticles of graphitic  $C_3N_4$  with different diameters and morphology could be immobilized inside the channels of mesoporous silica host matrices.<sup>22</sup> It has been also shown that the graphitic  $C_3N_4$  nanoparticle-immobilized mesoporous silica exhibits excellent photoluminescence properties.<sup>22</sup> However, by constructing CN materials with porous structure, many novel applications could emerge: from catalysis to separation and adsorption of very bulky molecules and the fabrication of low-dielectric devices. The synthesis of porous carbon nitride with a high nitrogen content is very difficult because of the greater thermodynamic stability of carbon and nitrogen molecules. Very recently, Vinu et al. have successfully reported the preparation of one-dimensional mesoporous CN (MCN-1) with a C:N atomic ratio of about 4:1 using SBA-15 as a template.<sup>23</sup> Unfortunately, this material possesses very low surface area, pore volume, and one-dimensional porous structure. Later, Goettmann et al. found that the mesoporous carbon nitride hybrid materials can be used as a metal-free catalyst for the Friedel–Crafts reaction of benzene and showed excellent catalytic activity.<sup>24</sup> Recently, Kaskel et al. have demonstrated the preparation of nitrogen-based mesoporous silicon oxynitride with different pore diameters by reacting silicon halides with gaseous ammonia in an organic solvent followed by sublimation of the byproducts in an ammonia flow and showed their superior performances in the base-catalyzed reactions.<sup>25,26</sup> This research confirms the potential of nitrogen-based mesoporous hybrid materials in many applications in various fields ranging from electrical and electronic to catalysis.

Mesoporous CN (MCN) hybrid materials with three-dimensional cage type pore systems promise access to an even wider range of application possibilities because of their unique properties such as semiconductivity, drug delivery, catalysis, etc.<sup>6–19</sup> More importantly, the accessibility of the pores and the surface active sites are easily achievable in the three-dimensional cage type porous structure. However, to the best of our knowledge, there are no reports on mesoporous carbon-nitride-based hybrid material having three-dimensional cage type pore structure with a well-defined pore size and morphology (MCN-2). Here, we report the preparation of such a novel material through the polymerization reaction between ethylenediamine and carbon tetrachloride using SBA-16 as the template. It has always been a challenge to get well-ordered mesoporous materials that are mainly carbon using SBA-16 as a template because of its porous structure. However, we optimized the synthetic procedure that was used in the synthesis of mesoporous carbon nitride using SBA-15 and could get a well-ordered three-dimensional mesoporous cage type carbon-nitride-based hybrid material. Interestingly, we found that the surface area,

**Scheme 1. Synthesis Procedure of Mesoporous Carbon-Nitride-Based Hybrid Material**



pore volume, and pore size of MCN-2 are much larger compared to that of MCN-1.

## Experimental Section

### Synthesis of Three-Dimensional Cage Type Mesoporous Silica

**Template, SBA-16.** Triblock copolymer Pluronic F127 ( $EO_{106}PO_{70}$ - $EO_{106}$ ,  $M_{av} = 12\,600$ ) was used as received from Sigma. Sodium metasilicate nonahydrate ( $Na_2SiO_3 \cdot 9H_2O$ ) and hydrochloric acid (c-HCl, 37.6%) were obtained from Fisher Scientific. In a typical synthesis, 16 g of a 10% aqueous solution of F127 was poured into 26.6 g of distilled water and then 4.71 g of sodium metasilicate ( $Na_2SiO_3 \cdot 9H_2O$ ) was added at 40 °C with magnetic stirring to yield a clear solution. To this solution was quickly added 13 g of concentrated hydrochloric acid (37.6%) with vigorous stirring to obtain a gel. The molar composition of the gel mixture was  $1.0:3.17 \times 10^{-4}:6.68:137.9$   $SiO_2:F127:HCl:H_2O$ . The gel solution was stirred for 24 h at 37 °C before being loaded into an autoclave and heated for 24 h at 100 °C. The solid product was filtered, dried at 120 °C overnight, and calcined in air at 500 °C.

**Synthesis of Three-Dimensional Mesoporous Carbon-Nitride-Based Hybrid Material.** Calcined SBA-16<sup>27</sup> (0.5 g) was added to a mixture of ethylenediamine (1.35 g) and carbon tetrachloride (2.31 g). The resultant mixture was refluxed and stirred at 90 °C for 6 h. The obtained dark brown colored solid mixture was then placed in a drying oven for 12 h and ground into a fine powder. The template-carbon nitride polymer composites were then heat-treated in a nitrogen flow of 50 mL per minute at 600 °C with a heating rate of 3.0 °C  $min^{-1}$  and kept under these conditions for 5 h to carbonize the polymer. The mesoporous carbon-nitride-based hybrid material (MCN-2) was recovered by filtration after dissolution of the SBA-16 silica framework in 5 wt % hydrofluoric acid, washed several times with ethanol, and dried at 100 °C. Scheme 1 summarizes the complete synthesis details of the MCN-2. It is important to note that when the synthesis procedure for the MCN-1 was used,<sup>20</sup> no solid product was obtained.

**Characterization.** The powder X-ray diffraction patterns of SBA-16 and MCN-2 materials were collected on a Rigaku diffractometer using  $Cu\ K\alpha$  ( $\lambda = 0.154$  nm) radiation. The diffractograms were recorded in the  $2\theta$  range of 0.8–10° with a  $2\theta$  step size of 0.01° and a step time of 1 s. Nitrogen adsorption and desorption isotherms were measured at -196 °C on a Quantachrome Autosorb 1 sorption analyzer. All samples were outgassed for 3 h at 250 °C under a vacuum ( $p < 1 \times 10^{-5}$  h Pa) in the degas port of the adsorption analyzer. The specific surface area was calculated using the BET model. The pore size distributions were obtained from both the adsorption and desorption branches of the nitrogen isotherms. The diameter of the cages in SBA-16 and MCN-2 was calculated using eq 1, which was recently proposed by Ravikovitch and Niemark<sup>28</sup>

$$D_{me} = a(6\epsilon_{me}/\pi\nu)^{1/3} \quad (1)$$

(21) Liu, A. Y.; Cohen, M. L. *Science* **1989**, *245*, 841.

(22) Groenewolt, M.; Antonietti, M. *Adv. Mater.* **2005**, *17*, 1789.

(23) Vinu, A.; Ariga, K.; Mori, T.; Nakanishi, T.; Hishita, S.; Golberg, D.; Bando, Y. *Adv. Mater.* **2005**, *17*, 1648.

(24) Goettmann, F.; Fischer, A.; Antonietti, M.; Thomas, A. *Angew. Chem., Int. Ed.* **2006**, *45*, 4467.

(25) Kaskel, S.; Schlichte, K.; Zibrowius, B. *Phys. Chem. Chem. Phys.* **2002**, *4*, 1675.

(26) Kaskel, S.; Schlichte, K. *J. Catal.* **2001**, *201*, 270.

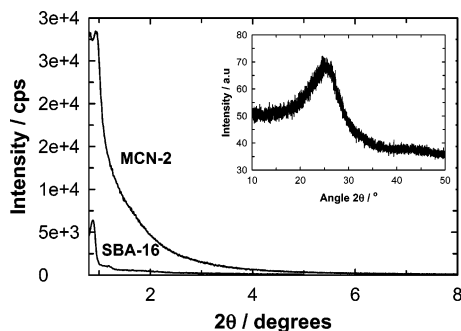


**Figure 1.** Powder XRD patterns of SBA-16 and MCN-2 (inset, higher-angle powder XRD pattern of MCN-2).

In eq 1,  $D_{me}$  is the diameter of the cavity of a cubic unit cell of length  $a$ ,  $\epsilon_{me}$  is the volume fraction of a regular cavity, and  $\nu$  is the number of cavities present in the unit cell (for the  $Im\bar{3}m$  space group,  $\nu = 2$ ).

The wall thickness of the cage type mesoporous materials was calculated using eq 2, which was derived from eq 1

$$h = 2a^3/\pi D_{me}^2 \nu - D_{me}/3 \quad (2)$$

The HRTEM images were obtained using JEOL-3000F and JEOL-3100FEF field-emission high-resolution transmission electron microscopes equipped with a Gatan-766 electron energy-loss spectrometer (EELS). The detailed experimental description about EELS measurement is given in the Supporting Information. The preparation of samples for HRTEM analysis involved sonication in ethanol for 2–5 min and deposition on a copper grid. The accelerating voltage of the electron beam was 200 kV. Elementary analysis was done using an Analyst AA 300 spectrometer. X-ray photoelectron spectroscopy (XPS) measurements were carried out in a PHI 5400 instrument with a 200 W Mg K $\alpha$  probe beam to characterize the samples. The spectrometer was configured to operate at high resolution with a pass energy of 20 eV. Prior to the analysis, the samples were evacuated at high vacuum and then introduced into the analysis chamber. Survey and multiregion spectra were recorded at C<sub>1s</sub> and N<sub>1s</sub> photoelectron peaks. Each spectra region of photoelectron interest was scanned several times to obtain good signal-to-noise ratios. The <sup>13</sup>C NMR spectrum was recorded on a Bruker spectrometer. Dipolar decoupling magic angle spinning (DD-MAS) sequence with the operating frequency of 75.49 MHz was used for obtaining the <sup>13</sup>C spectrum. Tetramethylsilane was used as a reference. FT-IR spectrum of MCN-2 was recorded on a Nicolet Nexus 670 instrument by averaging 200 scans with a resolution of 2 cm<sup>-1</sup> measuring in transmission mode using the KBr self-supported pellet technique. The spectrometer chamber was continuously purged with dry air to remove water vapor.

## Results and Discussion

Figure 1 shows the powder XRD pattern of MCN-2 along with the parent mesoporous silica, SBA-16. It can be seen that SBA-16 mesoporous silica template exhibits well-resolved (110), (200), and (211) reflections, characteristics of the body centered three-dimensional cubic space group  $Im\bar{3}m$ . The powder XRD pattern of MCN-2 also shows a sharp low-angle peak and a broad higher-order peak and is almost similar to that obtained for the SBA-16 mesoporous silica template (Figure 1). The results indicate that the

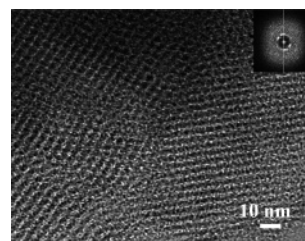


**Figure 2.** HRTEM image of MCN-2 and its corresponding fast Fourier transform (FFT) image.

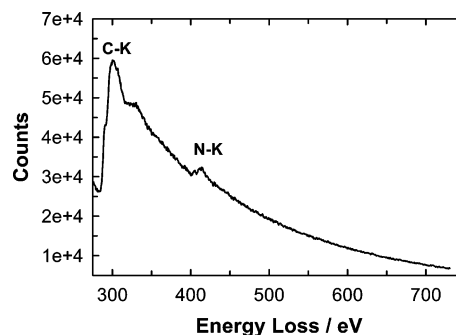


**Figure 3.** EEL spectrum of MCN-2.

material possesses a possible a three-dimensional mesoporous cage structure replicated from the template SBA-16. It is interesting to note that the intensity of the (110) peak of MCN-2 is much higher than that of the silica template. The unit-cell parameter of the MCN-2 is calculated using the formula  $2^{1/2}d_{110}$  to be 13.4 nm. The higher angle powder diffraction pattern of MCN-2 is also shown in Figure 1B. The samples exhibits a single broad diffraction peak (inset) near 25.47° ( $d = 3.42$  Å). This peak is almost similar to the characteristic 002 basal plan diffraction peak in the nonporous carbon nitride spheres. This reveals the presence of turbostratic ordering of the carbon and nitrogen atoms in the graphene layers of MCN-2.

The HRTEM image of MCN-2 taken along [110], in which the bright contrast strips on the image represent the pore wall images, whereas dark contrast cores display empty channels (see Figure 1S in the Supporting Information), shows a well-ordered mesoporous structure with a regular intervals of linear array of mesopores throughout the samples, which is characteristic of well-ordered SBA-16 mesoporous silica. Figure 2 clearly shows the presence of well-ordered domains of three-dimensional cubic mesoporous structure of the MCN-2 sample, which is almost similar to the structure of SBA-16. The corresponding fast Fourier transform pattern is shown in Figure 2 (inset), which can be attributed to the [110] axis of the cubic MCN-2 material. On the basis of the HRTEM image and the FFT pattern, the occurrence of well-ordered mesopores with a possible three-dimensional cubic mesoporous structure in MCN-2 is suggested here, which is consistent with the XRD results and suggests the possible replicated synthesis of the three-dimensional carbon nitride from SBA-16.

The electron energy loss spectrum (EELS) exhibits C and N K-edges located at 286 and 403 eV (Figure 3). The peak at 286 eV is due to transitions from the orbital  $1s-\pi^*$  states, which is mainly caused by the higher electronegativity of nitrogen that decreases the electron density on the C atoms.<sup>9</sup>

(27) Kim, J. M.; Sakamoto, Y.; Hwang, Y. K.; Kwon, Y.-U.; Terasaki, O.; Park, S.-E.; Stucky, G. D. *J. Phys. Chem. B* **2002**; *106*, 2552.

(28) Ravikovitch, P. I.; Neimark, A. V. *Langmuir* **2002**, *18*, 1550.



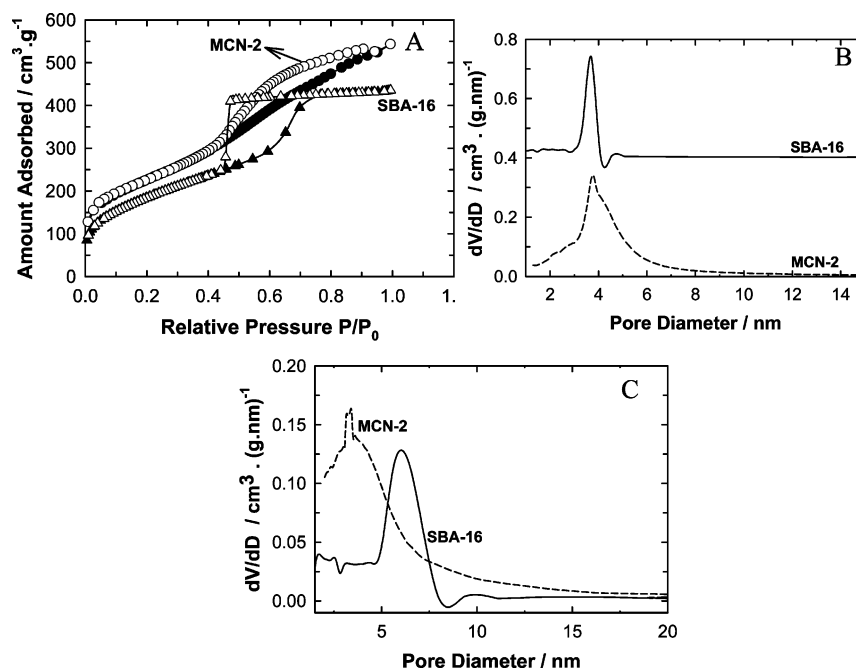


**Figure 4.** Nitrogen adsorption–desorption isotherms (A), and BJH desorption (B) and adsorption (C) pore size distributions of SBA-16 and MCN-2 (closed symbols, adsorption; open symbols, desorption).

**Table 1. Textural Parameters of MCN-2, SBA-16, MCN-1, and SBA-15**

materials	$a_0$ (nm)	specific surface area (m <sup>2</sup> /g)	pore volume (cm <sup>3</sup> g <sup>-1</sup> )	cage diameter (nm) <sup>22</sup>	wall thickness (nm) <sup>22</sup>	BJH pore diameter (nm)
MCN-2	13.40	810	0.81	10.83	2.91	3.45 (3.8) <sup>a</sup>
SBA-16	14.19	750	0.65	11.33	3.30	5.70 (3.7) <sup>a</sup>
MCN-1 <sup>20</sup>	9.52	505	0.55		4.52	4.0
SBA-15 <sup>20</sup>	10.30	910	1.20		1.30	9.0

<sup>a</sup> The number in parentheses indicates the BJH desorption pore diameter.

The fine structure of the C K-edges is assigned to trigonal sp<sup>2</sup>-hybridized C bonded to N. The N K-edge of the CN sample at 403 eV also indicates that the nitrogen atoms in the MCN-2 material are mostly sp<sup>2</sup> hybridized, in agreement with the conclusions from the analysis of the C K edge.<sup>9</sup> It is worthwhile to note that the EEL spectrum does not show any peak above 500 eV, indicating that the sample is mainly composed of C and N. Figures 2S in the Supporting Information shows the elemental mapping of C and N atoms in the MCN-2 sample. The data reveal that the carbon (C) and nitrogen (N) (see Figure 2S in the Supporting Information) are uniformly distributed throughout the sample. No other elements was found in the elemental mapping, indicating that the material is mainly composed of C and N. The C:N ratio of MCN-2 calculated from the EELS is ca. 4, which is in close agreement with the value obtained from CHN analysis, i.e., 4.1 (see Table 1S in the Supporting Information). It can be seen from Table 1S that 2.1% H and 5.4% other elements (probably Si, O, Cl, or F) are present in the MCN-2 after the silica removal. The trace of H comes from either the moisture or ethanol adsorbed on the surface or NH group on the MCN-2 matrix, whereas the presence of oxygen in the sample is due to the moisture or CO<sub>2</sub> adsorbed on the surface of MCN-2.

The nitrogen adsorption isotherm of MCN-2 in comparison to that of the parent silica template is shown in Figure 4A. Both the materials exhibit type IV isotherm with a broad H<sub>2</sub> hysteresis loop at the high relative pressure region, which is

typical for the well-ordered large cage type mesoporous material. The amount of nitrogen adsorbed on the MCN-2 sample is much higher than that of the parent mesoporous silica template. As can be seen from Figure 4A, MCN-2 features a broader capillary condensation step than that of its parent silica, indicating a slight disorder in the porous matrix in the MCN-2. From Table 1, it can also be seen that the specific surface area and the specific pore volume of MCN-2 are much higher than those of the template and the one-dimensional mesoporous carbon nitride, MCN-1, prepared from the one-dimensional mesoporous silica template, SBA-15.<sup>23</sup> The wall thickness and cage diameter of MCN-2 are lower than those of its parent silica template. This could be mainly due to the incomplete filling of carbon and nitrogen sources in the cages of SBA-16 silica template. It is also important to note that no well-ordered cage type mesoporous carbon nitride was obtained when our previous synthesis procedure for MCN-1 was used in this study. This could mainly be attributed to the difference in the pore structure and the diameter of SBA-16 as compared to those of SBA-15 template. To the best of our knowledge, this is the first report on the preparation of three-dimensional cage type mesoporous carbon nitride materials with a very high specific surface area and specific pore volume, which are crucial for the applications in adsorption and fuel cells. The BJH adsorption and desorption pore distributions of MCN-2 along with its parent mesoporous silica are shown in panels B and C of Figure 4, respectively. Although the pore diameter

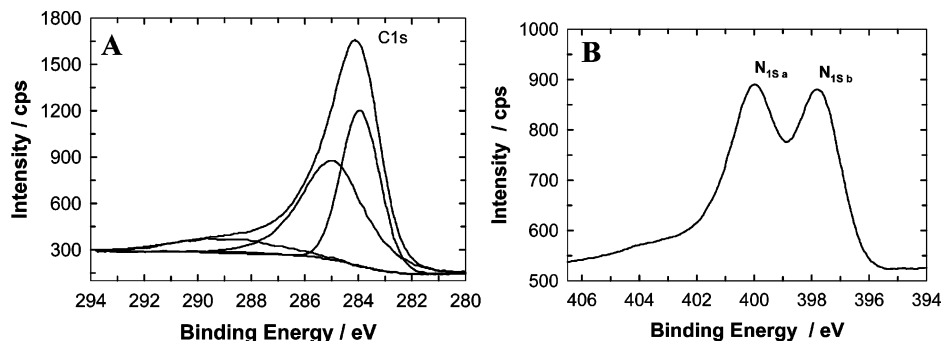


Figure 5. Core level C1s (A) and N1s (B) spectra of MCN-2.

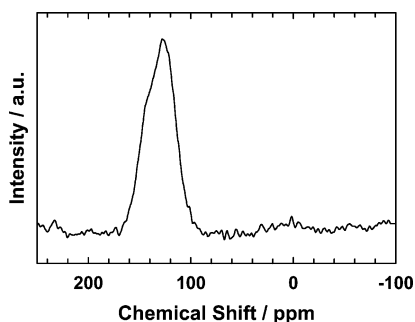


Figure 6.  $^{13}\text{C}$  DD-MAS spectrum of MCN-2.

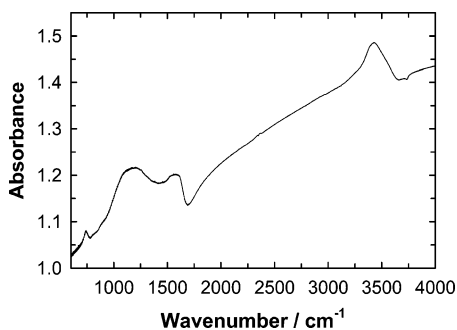
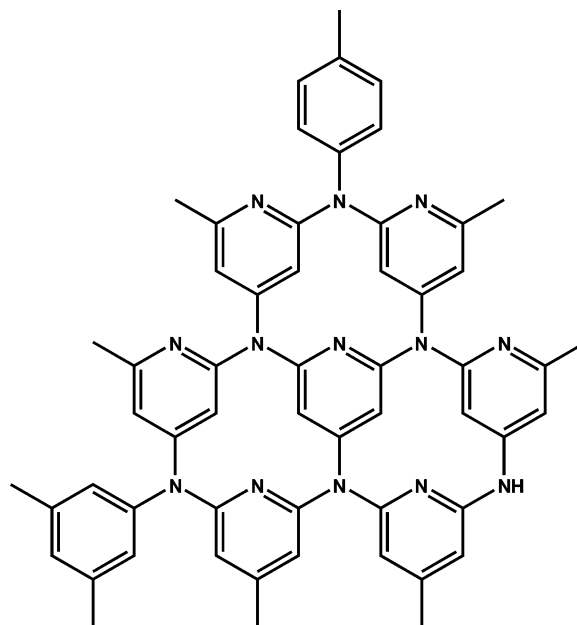


Figure 7. FT-IR spectrum of MCN-2 material.

of the MCN-2 is almost similar to that of SBA-16, the pore size distribution of MCN-2 is a little bit broader than that of the SBA-16. This could be attributed to a slight mesostructural disorder in the MCN-2 materials, mainly because of the incomplete filling of the CN polymer matrix inside the pores of the silica template.

The nature, chemical composition, and purity of the MCN-2 were obtained by XPS and FT-IR spectroscopic measurements. The XPS survey spectrum shows the presence of C, N, and O (see Figure 3S in the Supporting Information). The presence of a little amount of oxygen can be attributed to the moisture, ethanol, atmospheric  $\text{O}_2$ , or  $\text{CO}_2$  adsorbed on the surface of MCN-2. The overall atomic carbon to nitrogen ratio of MCN-2 determined by XPS is found to be 4.15, which is in close agreement with the results obtained from EELS and CHN analysis. Figure 5A shows the high-resolution C1s and N1s spectra of MCN-2. The C1s spectra could be deconvoluted into three well-resolved peaks with binding energies of 284.0, 285, and 288.8 eV, which were very close to the reported binding energy values of nonporous carbon nitride samples.<sup>8–12</sup> The peak at 284.0 and 285.0 eV are assigned to graphitic sites in the amorphous CN matrix and  $\text{sp}^2$  carbon atom bonded to N inside the aromatic ring,

Scheme 2. Schematic Structure of Mesoporous Carbon-Nitride-Based Hybrid Material



respectively, whereas the peak at 288.8 eV is attributed to the  $\text{sp}^2$ -hybridized carbon in the aromatic ring attached to the  $\text{NH}_2$  group.<sup>8–12</sup> The N1s spectra show two peaks centered at 397.7 and 400.0 eV, which could be attributed to N atoms trigonally bonded to all  $\text{sp}^2$  carbons and nitrogen  $\text{sp}^2$ -bonded to carbon, respectively.<sup>7,11,12</sup>

Figure 6 shows the  $^{13}\text{C}$  DD-MAS spectrum of the MCN-2 sample. The spectrum exhibits a sharp peak with a shoulder and could be deconvoluted into two well-resolved peaks with chemical shifts of 126 and 142 ppm. The peak at 126 ppm could be assigned for  $\text{sp}^2$  carbon atoms as such in graphitic carbon layers, whereas the peak at 142 ppm is attributed to the  $\text{sp}^2$  carbon atoms bonded to nitrogen as an aromatic ring attached to terminal  $\text{NH}_2$  groups.<sup>9,29</sup> To get a clear picture about the coordination of nitrogen in the MCN-2 materials, we tried to collect the  $^{15}\text{N}$  DD-MAS and  $^{15}\text{N}$  CP-MAS spectra. Unfortunately, only noisy spectrum was observed as the concentration of nitrogen in MCN-2 is low. The FT-IR spectrum of MCN-2 also reveals the existence of the CN matrix and shows four well-resolved bands centered at 742, 1209, 1560, and 3431  $\text{cm}^{-1}$  (Figure 7). The bands at 742, 1209, and 1560  $\text{cm}^{-1}$  are attributed to the  $\text{sp}^2$  graphitic sites,

(29) Li, D.; Chung, Y.-W.; Yang, S.; Wong, M.-S.; Adibi, F.; Sproul, W. D. *J. Vac. Sci. Technol., A* **1994**, *12*, 1470.

C–N stretching, and C=N stretching, respectively, whereas the band at 3431 is assigned to the residual NH or NH<sub>2</sub> components.<sup>6–19</sup> On the whole, the major IR characteristics bands are consistent with the general characteristics of other amorphous nonporous carbon nitride materials and MCN-1.<sup>23</sup> A schematic representation of the chemical structure of the MCN-2 is suggested with the help of the XPS, CHN, EELS, and IR data (Scheme 2).

### Conclusion

In summary, a highly ordered three-dimensional mesoporous carbon nitride material (MCN-2) with very high surface area, pore volume, and a possible cage type porous structure has been prepared using three-dimensional cage type meso-

porous silica, SBA-16, as a template through a simple polymerization reaction between ethylenediamine and carbon tetrachloride. The specific surface area and pore volume of MCN-2 are significantly higher compared to those of the template and MCN-1. Because of the excellent textural characteristic and three-dimensional porous structure, we believe that MCN-2 could offer great potential for the applications in catalysis and adsorption.

**Supporting Information Available:** Additional figures and experimental details of EELS analysis (PDF). This material is available free of charge via the Internet at <http://pubs.acs.org>.

CM070657K